

CMMLoc: Advancing Text-to-PointCloud Localization with Cauchy-Mixture-Model Based Framework

Yanlong Xu¹ Haoxuan Qu² Jun Liu² Wenxiao Zhang^{3†} Xun Yang^{1†}

¹ University of Science and Technology of China ² Lancaster University ³ Hohai University

kc30@mail.ustc.edu.cn, {h.qu5, j.liu81}@lancaster.ac.uk, wenxiao.zhang@gmail.com, xyang21@ustc.edu.cn

Abstract

The goal of point cloud localization based on linguistic description is to identify a 3D position using textual description in large urban environments, which has potential applications in various fields, such as determining the location for vehicle pickup or goods delivery. Ideally, for a textual description and its corresponding 3D location, the objects around the 3D location should be fully described in the text description. However, in practical scenarios, e.g., vehicle pickup, passengers usually describe only the part of the most significant and nearby surroundings instead of the entire environment. In response to this **partially relevant** challenge, we propose **CMMLoc**, an uncertainty-aware **Cauchy-Mixture-Model (CMM)** based framework for text-to-point-cloud **Localization**. To model the uncertain semantic relations between text and point cloud, we integrate CMM constraints as a prior during the interaction between the two modalities. We further design a spatial consolidation scheme to enable adaptive aggregation of different 3D objects with varying receptive fields. To achieve precise localization, we propose a cardinal direction integration module alongside a modality pre-alignment strategy, helping capture the spatial relationships among objects and bringing the 3D objects closer to the text modality. Comprehensive experiments validate that CMMLoc outperforms existing methods, achieving state-of-the-art results on the KITTI360Pose dataset. Codes are available in this GitHub repository <https://github.com/kevin301342/CMMLoc>.

1. Introduction

3D point cloud localization according to the given natural language descriptions, is promising in the future with the development of autonomous driving [13] and embodied agents [21], especially in large-scale urban environments. In practical scenarios, GPS performance often suffers due to signal blockage in certain environments, such as in urban

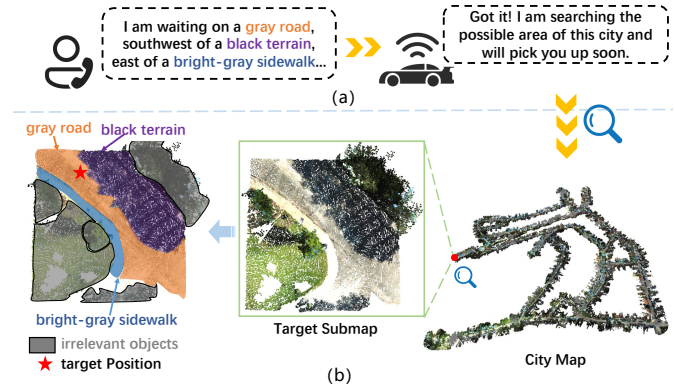


Figure 1. Given a text description of a location in (a), CMMLoc searches the 3D city and identifies the most likely target location of the described position within a submap in (b). Notably, text descriptions do not correspond to all objects within the submap, where the irrelevant objects are shown in gray color.

canyons [6, 41]. Conversely, language-based point cloud localization can help under these conditions. Furthermore, this technology offers significant convenience for humans, as it eliminates the need to provide an exact address, freeing us from the limitations of GPS tags and enabling more user-friendly human-machine interactions.

3D point cloud localization based on text descriptions is a challenging task due to the gap between linguistic descriptions and large-scale point clouds. To simplify this difficult task, the pioneering work Text2Pos [18] proposes a coarse-to-fine pipeline that divides the city map into submaps, first retrieving candidate submaps based on global descriptor matching, followed by fine localization through hint-to-instance correspondence. However, it does not account for the relationships within text queries or between point clouds. RET [42] improves cross-modal collaboration by introducing a Relation-Enhanced Transformer. Text2Loc [47] adopts a frozen pre-trained T5 [32] model and a hierarchical transformer to analyze the relationships between text descriptions with a matching-free regression method for fine localization.

While these approaches make significant progress on this

[†]Corresponding authors.

task, they overlook the *partial relevance characteristic* between text descriptions and the 3D objects in the scene. As is shown in Fig. 1, during vehicle pickup in (a), the ideal scenario would involve passengers providing a detailed and comprehensive description of all surrounding objects within the target submap in (b), including a gray road, a black terrain, a bright-gray sidewalk, and other irrelevant objects in gray color. However, passengers typically describe only the most significant and nearby surroundings like (a). This selective description introduces uncertainty into the text-to-3D object-matching process, potentially disrupting the semantic modeling between text and 3D objects.

Based on this observation, we propose CMMLoc, an uncertainty-aware text-to-point-cloud localization framework based on the Cauchy-Mixture-Model. Notably, CMM naturally adapts to partially relevant problems, where both relevant and irrelevant objects are present. This is because, as analyzed in [15], CMM has the property of diminishing the influence of irrelevant objects without entirely disregarding them. This aligns well with the expectations for partially relevant problems. Our framework employs a coarse-to-fine localization pipeline: initial text-submap retrieval, followed by fine localization. In the coarse submap retrieval stage, we propose a Cauchy-Mixture-Model-based Transformer to model 3D object representations. Inspired by advancements in the NLP field [17], we design a Cauchy weighted attention scheme, whose attention weights are attenuated according to the semantic similarity between correlated objects. Specifically, we initially utilize multi-scale Cauchy windows, which incorporate Cauchy distribution as priors, to model the semantic relationships among 3D point cloud objects to generate 3D object features with varying receptive fields. Subsequently, considering the sparsity and various shapes of point clouds, we propose an innovative spatial consolidation scheme that could adaptively aggregate the 3D object features with different receptive fields. In the fine localization stage, we incorporate a cardinal direction integration module combined with a cross-modality pre-alignment strategy. In particular, we first pre-align the multi-modal encoder to bring the 3D objects closer to the text modality. Then we design a Cardinal Direction Integration module to capture spatial relations among objects, which can encourage more fine-grained interactions between 3D objects and text queries.

We conduct extensive experiments on the KITTI360Pose dataset, demonstrating that our framework achieves state-of-the-art performance in cross-modal text-to-point-cloud localization. Additional experimental results further validate the necessity and correctness of modeling the partial relevance between text queries and 3D objects.

In summary, our main contributions are as follows:

- We deeply analyze the current coarse-to-fine pipeline for 3D language-based point cloud localization task and point

out the partially relevant characteristic of this task which was overlooked by previous work. To tackle this problem, we propose a novel framework CMMLoc.

- For the coarse stage, we introduce a Cauchy-Mixture-Model-based Transformer that incorporates CMM priors for 3D object modeling, along with a spatial consolidation scheme for better submap representation. For fine localization, we propose a pre-alignment strategy and a cardinal direction integration module to enhance cross-modality interactions, ultimately yielding improved localization accuracy.
- Extensive experiments on the KITTI360Pose dataset demonstrate the effectiveness of our approach, which achieves state-of-the-art performance.

2. Related Work

2D visual grounding. 2D visual grounding aims to estimate an accurate position based on a given image or image query. Traditional techniques cast this problem as an instance retrieval task and employ various aggregation methods to extract invariant image features and then perform objects matching across different viewpoints like Scale Invariant Feature Transform (SIFT) [24], Vector of Locally Aggregated Descriptors (VLAD) [2], Generalized-Mean (GeM) [31] and so on. Recent methods [35, 36] mostly adopt a coarse-to-fine localization pipeline. Given an image query, the coarse stage uses K-Nearest Neighbors to find candidate subsets, and the fine stage establishes pixel-wise correspondences between the query and candidates for precise position prediction. Compared to 2D visual grounding, our task is more challenging due to the huge gap between text descriptions and large-scale urban point clouds.

3D point cloud based place recognition. Point cloud-based place recognition is similar to 2D visual grounding, the difference lies in that the query of this task is a single scan from 3D LiDAR sensor rather than an image. Methods for this task can be divided into two categories: those based on global descriptors and those based on plane or object descriptors. Early works like [28, 34] use global statistics to construct handcrafted global descriptors. Representing the scan as the bird’s-eye view (BEV) is another popular approach. Scan Context [16], for example, computes a handcrafted descriptor from a BEV scan representation. Then deep learning of global descriptors becomes the focus of the research. The first notable method PointNetVLAD [38] combines PointNet [29] with NetVLAD [2] to aggregate local features into a global descriptor. Following methods like [8, 23, 37, 46, 49] focus on better feature combination. Transformer-based methods like [3, 7, 9, 26, 27, 51] utilize different transformer networks to enhance the performance. However, MinkLoc3D [19] employs sparse 3D convolution and outperforms transformer-based methods with fewer parameters. MinkLoc++ [20] further improves MinkLoc3D

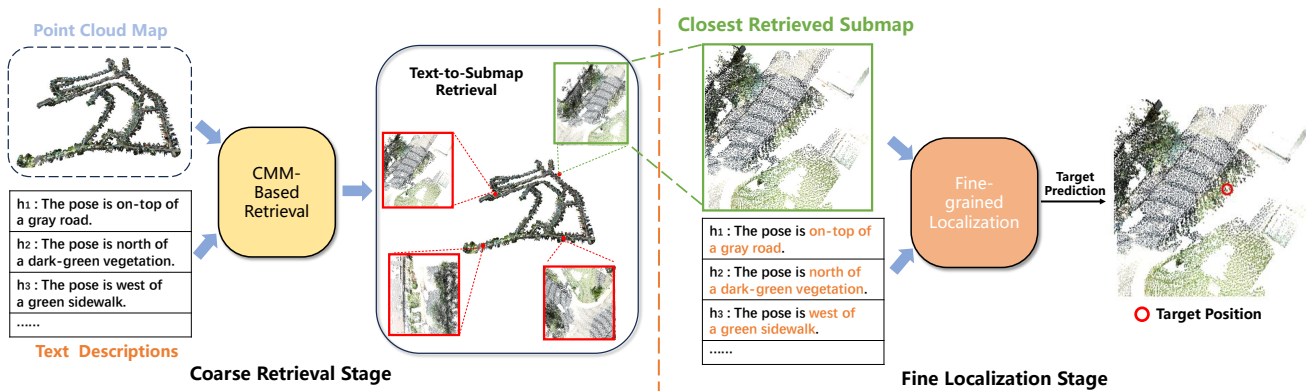


Figure 2. The overview of proposed CMMLoc. It is a coarse-to-fine architecture consisting of two stages: Coarse submap retrieval and Fine localization. *Coarse submap retrieval.* Given text descriptions, we first identify a set of candidate submaps potentially containing the target position. This is achieved by retrieving the Top-k nearest submaps from a constructed database of submaps using our CMM-based retrieval model. *Fine localization.* We then refine the coordinates of the retrieved submaps via our pre-alignment strategy and cardinal direction integration module to improve localization accuracy.

by incorporating the ECA [43] attention mechanism, similar to Transloc3D [48]. Recently, the re-ranking technique has been taken into consideration by researchers like [50] to boost efficiency. There also exist works like [10, 11] which propose to use 3D shapes or object-centric recognition as a different solution. By contrast to point cloud place recognition, our task uses linguistic descriptions as queries to locate the target position.

Text-guided point cloud localization. Given a 3D point cloud scene, text-guided point cloud localization refers to the task of semantically locating a target position based on language descriptions. It was first introduced in [1, 4]. Recent research in this area can be broadly classified into two categories: two-stage and one-stage frameworks. Two-stage frameworks like [5, 12, 33] first generate multiple proposals by the pre-trained 3D detector and then reason about detected proposals with text descriptions to output the final result. In contrast, one-stage methods like [14, 25, 45] take the whole 3D scene as input and directly regress the spatial bounding box of the text-guided object. However, most of these works focus on indoor scenes, whereas our work is concerned with large-scale outdoor scene localization. Text2Pos [18] is the first to formalize this task and introduce the first dataset along with a coarse-to-fine localization pipeline. RET [42] and Text2Loc [47] continue to improve the performance with their novel designs. In this work, we also follow the two-stage pipeline but emphasize the partial relevance characteristic of this task, which has been overlooked in previous studies.

3. Preliminaries

The task aims to find the most corresponding position (x, y) described by linguistic descriptions within the large-scale urban map M . To simplify this difficult task, we first divide the urban map into cubic submaps, denoted as $\{M_i\}_{i=1}^m$, where m represents the number of submaps. Each submap

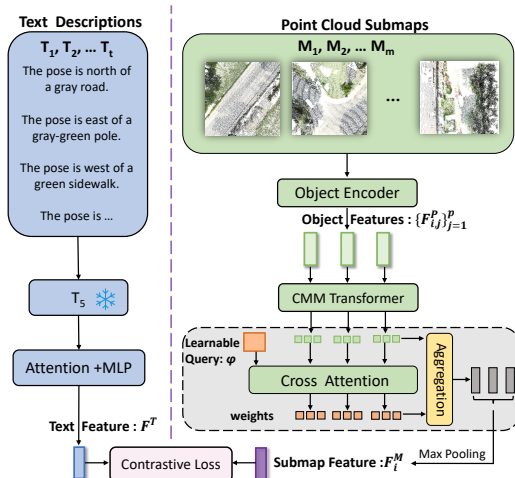


Figure 3. Illustration of coarse submap retrieval. We introduce the CMM Transformer and spatial consolidation scheme in the object encoding branch to model the partial relevance between 3D objects and achieve a better representation of the submap. Note that the T5 model in the text encoding branch is frozen during this process.

$M_i = \{P_{i,j} | j = 1, \dots, p\}$ consists of a set of object point clouds $P_{i,j} \in \mathbb{R}^{s \times 3}$, where s is the number of points in the object. Each object $P_{i,j}$ is obtained through semantic segmentation from the point cloud of the submap M_i . Besides, text query T is represented as a set of hints $\{h_t\}_{t=1}^h$, where each hint describes the spatial relationships between the target position and its surrounding objects.

4. Method

We adopt a coarse-to-fine pipeline [18, 47] and propose a novel framework CMMLoc to address the language-based point cloud localization problem as shown in Fig. 2. In the coarse stage, the goal of the task is to identify the submap most likely to contain the target position. Recognizing the partially relevant nature of this task, we design a Cauchy-

Mixture-Model-based Transformer and a spatial consolidation scheme for better representation of submaps, as detailed in Sec. 4.1. In the fine stage, we focus on locating the target position based on T and retrieved candidate submaps. We first pre-align text and object features via pre-training to bring 3D objects closer to the text modality, and then we introduce a cardinal direction integration module to capture the spatial relationships among objects for more fine-grained interactions between two modalities, described in Sec. 4.2. Training loss functions are described in Sec. 4.3.

4.1. Coarse text-submap retrieval

Following [18, 42, 47], we employ a dual branch to learn global descriptors of text query T and submap M_i as is shown in Fig. 3. Previous works solve this problem by matching the extracted global descriptors of text query and object point clouds, but they overlook the *partially relevant characteristic* between the text descriptions and 3D objects in the submap. This oversight can degrade the global representation and lead to suboptimal submap retrieval performance. To address this, we formulate the coarse stage as a partially relevant retrieval problem and introduce a Cauchy-Mixture-Model-based Transformer in the submap encoding branch. Additionally, we propose a spatial consolidation scheme to improve submap representation.

Text encoder. Given a text query, we first extract its features using the frozen pre-trained model T5 [32], which can help to get good initial embeddings due to the extensive pre-trained knowledge in T5. Next, we utilize the attention mechanism [40] to capture the contextual relationships between words and sentences. Specifically, we feed the text embeddings into the transformer block that involves multi-head self-attention and multi-layer perceptron (MLP) layers. This approach enables us to obtain better global descriptors of text query F^T , which pays attention to both the overall semantic meaning and the details.

Object encoder. To get the global descriptor of submap M_i , we adopt the approach that we encode every object $P_{i,j}$ in the submap and then aggregate the features to represent the submap. We first encode each object with PointNet++ [30] to get the semantic embedding. However, semantic features alone are not sufficient, as each object also has distinctive properties like color, position, and point number. Therefore, we use separate encoders for color, position, and point number, each consisting of a 3-layer MLP with the same embedding dimension as the semantic embedding. We then concatenate the embeddings from all encoders to form the initial representation of each object in the submap.

Cauchy-Mixture-Model-based Transformer. Previous works typically use the output of the object encoder as the final object embedding and aggregate them to represent the submap, which neglects the partially relevant property. To better model the entire submap, we feed the ob-

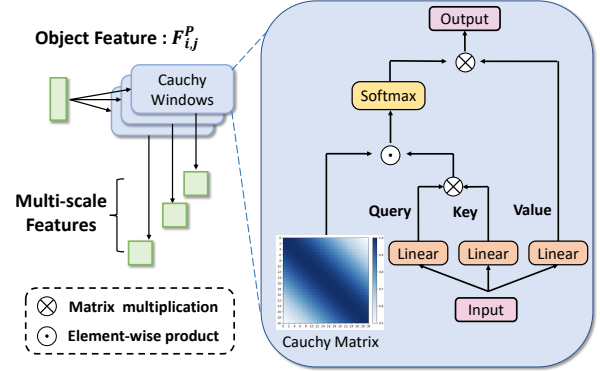


Figure 4. Illustration of CMM Transformer.

ject embeddings into our proposed Cauchy-Mixture-Model based Transformer (CMMT) inspired by [17, 44]. Specifically, CMMT is composed of several Cauchy windows, which incorporate Cauchy-Mixture-Model priors in the encoding process to encourage semantic similarity modeling as shown in Fig. 4. Given object features $\{F_{i,j}^P \in \mathbb{R}^d\}_{j=1}^p$ in submap M_i , we first represent them as a matrix $X_i \in \mathbb{R}^{p \times d}$. In the Cauchy window, we project X_i to query, key, value matrix W^q, W^k, W^v through learnable parameters. We then use the query matrix to perform scaled dot-product attention over the key matrix, yielding an attention matrix score. Finally, we apply a Cauchy matrix $W^c \in \mathbb{R}^{p \times p}$ to perform element-wise product over the attention scores:

$$X_i^{attn} = \text{Softmax}(W^c \odot \frac{X_i W^q (X_i W^k)^\top}{\sqrt{d_k}}) X_i W^v, \quad (1)$$

$$W^c(i, j) = \frac{1}{\pi \gamma [1 + (\frac{j-i}{\gamma})^2]}, \quad (2)$$

where d_k is the dimension of queries and keys, γ is the scale parameter of Cauchy density distribution and \odot indicates the element-wise product function. After obtaining X_i^{attn} , we pass it through a Feed-Forward Network (FFN) to get the output of the Cauchy window X_i^{output} . We have N parallel Cauchy windows with different scales as objects in every submap are various.

The Cauchy window is designed to effectively model local relationships among 3D objects by assigning different Cauchy weights within the feature matrix X_i . In other words, the order of object features is significant as adjacent features receive higher Cauchy attention weights. We explore two approaches for Cauchy matrix values assignment: one based on physical spatial distance and the other based on semantic similarity. Distance-based assignment means objects positioned closer get higher Cauchy weights, and assignment by semantic similarity means greater semantic similarity yields higher weights. Experiments in Sec. 5.3 prove that the distance-based approach is less effective. Therefore, we adopt semantic similarity for weight

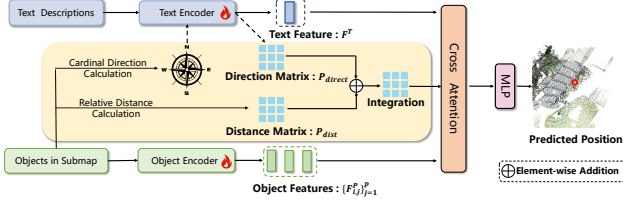


Figure 5. Illustration of Cardinal Direction Integration.

assignment. To implement this, we cluster the object features according to their semantic labels which are obtained during submap semantic segmentation, yielding object feature clusters $\{C_k\}_{k=1}^K$. These clusters are then randomly sorted to form the feature matrix X_i . Although random sorting is not optimal, we find that it yields comparable performance due to the heavy-tailed properties of the Cauchy distribution. Unlike Gaussian windows, the Cauchy window assigns higher probabilities to objects that are farther apart, making it more robust to outliers and better suited for modeling phenomena with unpredictable elements. A comparative analysis of the Cauchy and Gaussian distributions is presented in Sec. 5.3

Notably, in practical scenarios, misclassification can occur during the semantic segmentation process, which can affect the performance of our CMMLoc, as it relies on the semantic labels of the objects. To evaluate the robustness of CMMLoc under such conditions, we conduct an ablation study examining its performance under varying misclassification rates, as detailed in Sec. 5.3.

Spatial Consolidation Scheme. Considering the irregularity of the point cloud, we design a learnable query φ to learn adaptive aggregation weights for aggregating object features with varying receptive fields. In particular, we use a cross-attention layer to generate aggregation weights:

$$w_n = \text{Linear}\left(\text{Softmax}\left(\frac{\varphi X_{i,n}^{\text{output}}}{\sqrt{d_k}}\right) X_{i,n}^{\text{output}}\right), \quad (3)$$

$$\tilde{X}_i^{\text{output}} = \sum_{n=1}^N w_n X_{i,n}^{\text{output}}, \quad (4)$$

where n represents the index of the Cauchy window. After obtaining the object features in the submap, we apply a max pooling operation to obtain the final global descriptor of submap F_i^M for the partially relevant retrieval.

4.2. Fine localization

Following [47], we adopt a matching-free network as the base model for fine localization. Unlike the coarse stage, the key challenge in the fine stage is to encourage fine-grained interactions between the text queries and 3D objects in the submap. To this end, we propose a strategy: we first pre-align the text encoder and object encoder to bring 3D object features closer to the text modality. Then we introduce a

Cardinal Direction Integration method to capture the spatial relations between objects in the submap as a supplement for common positional embedding.

Pre-alignment. The main challenge in this task lies in the huge gap between the text modality and object point clouds, which hinders fine-grained alignment. To bridge this gap and make 3D objects more “language-like”, we pre-train both the text encoder and object encoder before training the model for localization refinement. Since the object labels and colors are the most relevant textual information for 3D objects, we involve the color encoder, the object encoder, and the text encoder for pre-alignment. Specifically, the color encoder and object encoder extract color embeddings F_{color}^P and object features F_{object}^P from the object point cloud, while the text encoder encodes the color and label information in the text query to produce text embeddings F_{color}^T and F_{label}^T . To provide a good initialization for the fine stage and facilitate better alignment, we aim to minimize the distance of matched embeddings, as is outlined in the loss function in Sec. 4.3.

Cardinal Direction Integration. The position encoder in the object encoder extracts the absolute position embedding of objects within the submap, but we believe this is insufficient for the fine-grained alignment between texts and objects. To address this, we introduce a Cardinal Direction Integration (CDI) module to capture the spatial relations between objects as illustrated in Fig. 5. Specifically, we compute the pair-wise distances between the center coordinates of objects in the submap, resulting in a distance matrix $P_{dist} \in \mathbb{R}^{p \times p}$. Additionally, we determine the relative cardinal direction between pairs of objects. For example, if object A is situated to the east of object B, the cardinal direction “east” is extracted. This textual directional information “east” is then encoded by the text encoder and fed into an MLP to form the direction matrix $P_{direct} \in \mathbb{R}^{p \times p}$. We combine both the distance and direction matrices to form the complete relative position matrix $P \in \mathbb{R}^{p \times p}$:

$$P = P_{direct} + \alpha * P_{dist}, \quad (5)$$

where α is a weight factor. Then we add the relative position matrix to the computed attention weights before doing the softmax in the attention layer. Considering the input for an attention layer: queries Q of size $p \times d_f$, keys K of size $p \times d_f$ and values V and the relative position matrix P , the output of the attention layer is:

$$A = \frac{QK^\top + P}{\sqrt{d_f}}. \quad (6)$$

Finally, we obtain the predicted position by passing the output of the attention layer through an MLP.

4.3. Loss Functions

For the coarse stage, given a batch of global descriptors of submaps $\{F_i^M\}_{i=1}^B$ and text queries $\{F_i^T\}_{i=1}^B$, where B

Methods	Localization Recall ($\epsilon < 5/10/15m$) \uparrow					
	Validation Set			Test Set		
	$k = 1$	$k = 5$	$k = 10$	$k = 1$	$k = 5$	$k = 10$
Text2Pos [18]	0.14/0.25/0.31	0.36/0.55/0.61	0.48/0.68/0.74	0.13/0.21/0.25	0.33/0.48/0.52	0.43/0.61/0.65
RET [42]	0.19/0.30/0.37	0.44/0.62/0.67	0.52/0.72/0.78	0.16/0.25/0.29	0.35/0.51/0.56	0.46/0.65/0.71
Text2Loc [47]	0.37/0.57/0.63	0.68/0.85/0.87	0.77/0.91/0.93	0.33/0.48/0.52	0.61/0.75/0.78	0.71/0.84/0.86
CMMLoc (Ours)	0.44/0.62/0.68	0.75/0.88/0.90	0.83/0.93/0.95	0.39/0.53/0.56	0.67/0.80/0.82	0.77/0.87/0.89

Table 1. Performance comparison on the KITTI360Pose benchmark [18].

Methods	Submap Retrieval Recall \uparrow					
	Validation Set			Test Set		
	$k = 1$	$k = 3$	$k = 5$	$k = 1$	$k = 3$	$k = 5$
Text2Pos [18]	0.14	0.28	0.37	0.12	0.25	0.33
RET [42]	0.18	0.34	0.44	-	-	-
Text2Loc [47]	0.32	0.56	0.67	0.28	0.49	0.58
CMMLoc (Ours)	0.35	0.61	0.73	0.32	0.53	0.63

Table 2. Performance comparison for coarse text-submap retrieval on the KITTI360Pose benchmark [18]. Note that only values that are available in RET [42] are reported.

represents the batch size, we employ contrastive loss between each pair to train our model instead of the pairwise ranking loss in previous work:

$$l(i, T, M) = -\log \frac{\exp(F_i^T \cdot F_i^M / \tau)}{\sum_{j \in N} \exp(F_i^T \cdot F_j^M / \tau)} - \log \frac{\exp(F_i^M \cdot F_i^T / \tau)}{\sum_{j \in N} \exp(F_i^M \cdot F_j^T / \tau)}, \quad (7)$$

where τ represents the temperature coefficient. Within a training batch, the final contrastive loss is computed by summing $l(i, T, M)$ and dividing by the batch size.

As for the fine stage, the objective of the fine stage is to minimize the difference between the predicted position and the ground truth. We take the strategy which includes pre-training first and then incorporate Cardinal Direction Integration for more fine-grained alignment. Specifically, we first use mean squared error loss for pre-alignment to make 3D objects more “like” language:

$$L_{pre} = \|F_{color}^P - F_{color}^T\|_2 + \|F_{object}^P - F_{label}^T\|_2, \quad (8)$$

then we continue to use the mean squared error loss to train the translation regressor:

$$L(P_{gt}, P_{pred}) = \|P_{gt} - P_{pred}\|_2, \quad (9)$$

where $P_{pred} = (x, y)$ is the coordinate of predicted position, and P_{gt} is the ground truth coordinates.

5. Experiments

5.1. Dataset & Evaluation metrics

We conduct our experiments including training and evaluating on the KITTI360Pose dataset [18], which is built upon

Methods	Submap Retrieval Recall \uparrow					
	Validation Set			Test Set		
	$k = 1$	$k = 3$	$k = 5$	$k = 1$	$k = 3$	$k = 5$
Transformer [47]	0.32	0.56	0.67	0.28	0.49	0.58
GMMFormer [44]	0.33	0.57	0.68	0.30	0.50	0.60
CMMT	0.33	0.58	0.69	0.31	0.52	0.62
CMMT-SC	0.35	0.61	0.73	0.32	0.53	0.63

Table 3. Ablation study of coarse text-submap retrieval on the KITTI360Pose benchmark [18]. Transformer indicates the attention mechanism in [47]. GMMFormer indicates the Gaussian-Mixture-Model-based Transformer designed for partially relevant video retrieval in [44]. CMMT denotes the Cauchy-Mixture-Model-based Transformer we propose. CMMT-SC refers to CMMT with the spatial consolidation scheme.

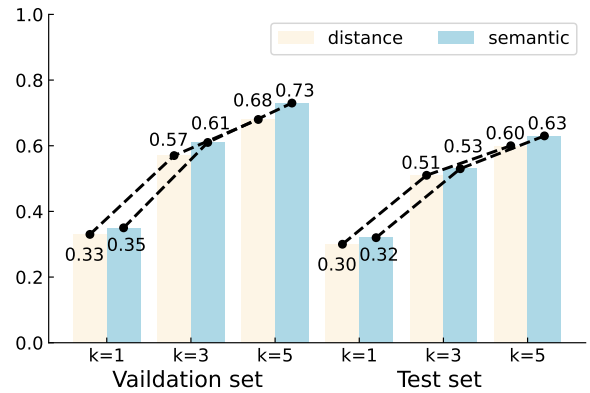


Figure 6. Performance comparison of coarse submap retrieval with different CMM weight allocation strategies on the KITTI360Pose dataset [18].

the KITTI360Pose dataset by [22] with sampled locations and generated hint descriptions. It contains point clouds of 9 urban scenes, covering 14,934 positions and 43,381 position-query pairs with an area of 15.51 km² in all. We follow the setting in [18] and choose 5 scenes for training, 1 scene for validation, and 3 scenes for testing. Each submap is a 3D cube with a fixed size of 30m and a stride of 10m. The whole dataset has 11,259/1,434/4,308 submaps for training/validation/testing scenes and 17,001 submaps in all.

We formulate the coarse stage as a partially relevant re-

Methods	Localization Recall ($\epsilon < 5m$) \uparrow					
	Validation Set			Test Set		
	$k = 1$	$k = 5$	$k = 10$	$k = 1$	$k = 5$	$k = 10$
Text2Loc [47]	0.37	0.68	0.77	0.33	0.61	0.71
Text2Loc*	0.42	0.74	0.83	0.37	0.65	0.74
CMMLoc_PA	0.43	0.74	0.83	0.38	0.66	0.75
CMMLoc_CDI	0.43	0.73	0.81	0.38	0.66	0.76
CMMLoc (Ours)	0.44	0.75	0.83	0.39	0.67	0.77

Table 4. Ablation study of fine localization on the KITTI360Pose benchmark. Text2Loc* indicates the fine localization network from Text2Loc, with submaps retrieved through our coarse model. CMMLoc_PA indicates the removal of the CDI while retaining the Pre-alignment process in our network. Conversely, CMMLoc_CDI keeps the CDI but removes the Pre-alignment.

retrieval problem and evaluate its performance using retrieval recall at Top k ($k \in \{1, 3, 5\}$). For fine localization, we utilize localization recall to assess localization capability. Specifically, based on the Top k retrieval candidates ($k \in \{1, 5, 10\}$), we measure the ratio of successfully localized queries if the error is below specific error thresholds, namely, $\epsilon < 5/10/15m$ by default.

5.2. Comparison with State-of-the-art Methods

Compared to existing methods, our method achieves the best performance, demonstrating its superiority. We evaluate the performance of our model on the KITTI360Pose validation and test sets for a fair comparison. For coarse submap retrieval, we report the results in Tab. 2. As shown, our model significantly outperforms previous methods. On the validation set, our best performance achieves a Top-1 recall of 0.35, exceeding the current state-of-the-art Text2Loc by 9%. On the test set, recall rates achieved at Top-1, Top-3, and Top-5 are 0.32, 0.53, and 0.63, respectively, improving on Text2Loc by 14%, 9%, and 8%. For fine localization, the results are shown in Tab. 1. We achieve a Top-1 recall rate of 0.44 on the validation set and 0.39 on the test set under an error bound of $\epsilon < 5m$, which are 19% and 18% higher than Text2Loc, respectively. Our method also maintains superior performance when relaxing the localization error constraints or increasing k .

5.3. Ablation study

In this section, we conduct ablation studies to evaluate the effectiveness of the proposed modules in CMMLoc for coarse submap retrieval and fine localization stages.

Coarse text-submap retrieval. For the coarse stage, our focus is on assessing the contribution of the proposed Cauchy-Mixture-Model-based Transformer and spatial consolidation scheme. As we are the first to formulate the sub-task in the coarse stage as a partially relevant retrieval problem, we compare CMMT with GMMFormer proposed in [44] and Transformer architecture used

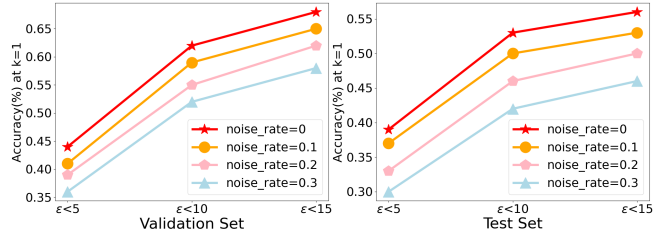


Figure 7. Performance Comparison at varying noise rates of the predicted object labels on the validation and test sets.

in Text2Loc [47]. As is illustrated in Tab. 3, GMMFormer [44], which was originally designed for partially relevant video retrieval, outperforms the Transformer architecture. This demonstrates the necessity of modeling the coarse stage as a partially relevant retrieval problem from a different perspective. Benefiting from the robust nature of the Cauchy distribution, CMMT is more resilient to outliers in the submap, contributing to better performance compared to GMMFormer. With the spatial consolidation scheme, CMMT becomes more adaptive to different 3D shapes and achieves superior results. In comparison with the Transformer used in Text2Loc, CMMT-SC achieves 0.35 at Top-1 on the validation set and 0.32 at Top-1 on the test set, outperforming the Transformer by margins of 9% and 14%, respectively. Based on the above analysis, we demonstrate the correctness of modeling the coarse stage as a partially relevant retrieval problem and the superiority of the proposed Cauchy-Mixture-Model-based Transformer and spatial consolidation scheme.

Moreover, we explore two different Cauchy weight assignment methods: distance-based and semantic similarity-based. The performance comparison on the KITTI360Pose dataset is shown in Fig. 6. As shown, assigning Cauchy weights based on semantic similarity performs better on both the validation and test sets, demonstrating the effectiveness of weighting according to semantic similarity. Furthermore, we consider practical scenarios where semantic labels are not readily available and require the pre-processing step of semantic segmentation. Under this circumstance, we investigate the impact of incorrect semantic labels on the performance of our model. Specifically, we add noise to the labels of the validation and test sets to simulate errors in semantic segmentation and then use the noisy dataset to evaluate the performance of our model. As is shown in Fig. 7, the performance of CMMLoc decreases as the noise rate increases, demonstrating its reliance on semantic labels. Notably, at a noise rate of 0.1, CMMLoc still outperforms Text2Loc [47], and at a noise rate of 0.2, its performance remains comparable, indicating the robustness of our method.

Fine localization. To validate the effectiveness of the Pre-alignment and Cardinal Direction Integration Module in the fine localization stage, we separately conduct abla-

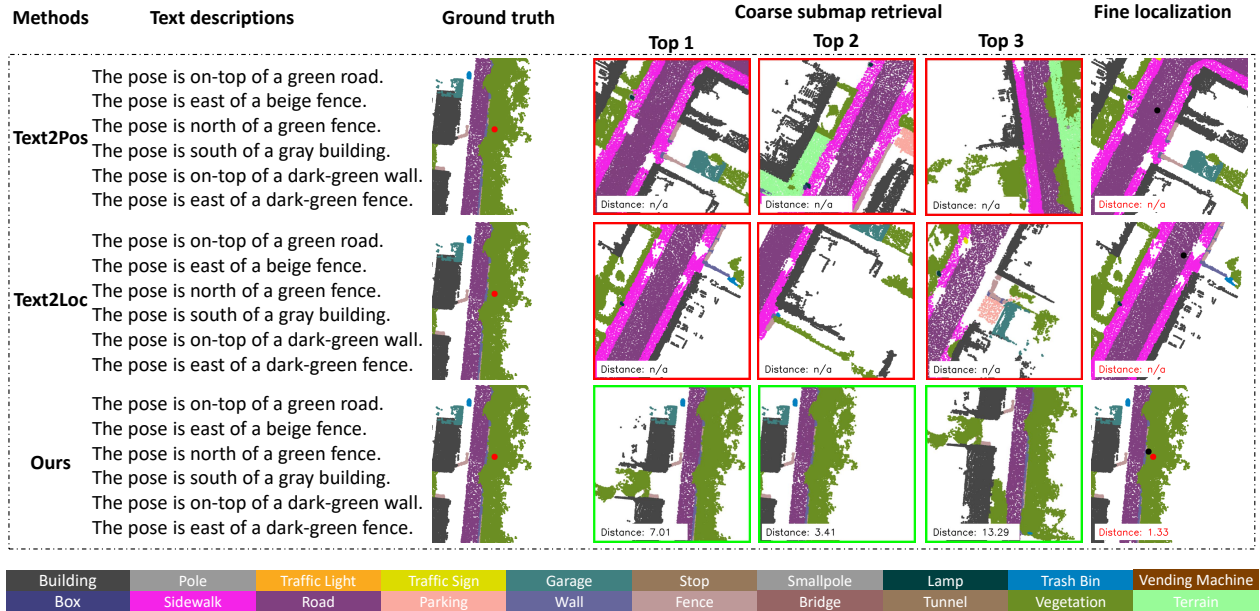


Figure 8. Qualitative localization results on the KITTI360Pose dataset: In coarse submap retrieval, green boxes indicate positive submaps containing the target location, while red boxes represent negative submaps. For fine localization, red and black dots correspond to the ground truth and predicted target locations. We label the distances between the prediction and ground truth in the submap, with “n/a” indicating submaps from different scenes.

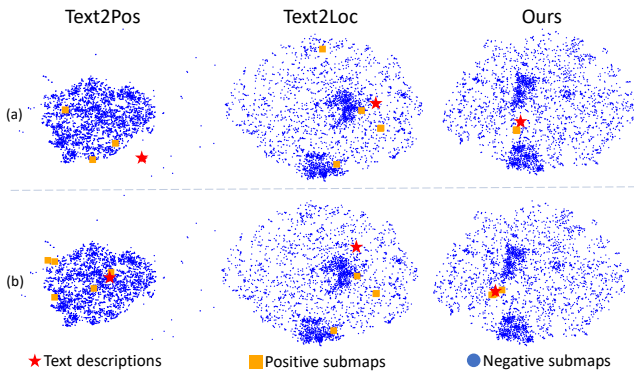


Figure 9. T-SNE visualization for coarse submap retrieval.

tion studies on them, denoted as CMMLoc_PA and CMMLoc_CDI. To fairly assess the results, we use the submaps retrieved from our coarse stage and report the results in Tab. 4. As shown, Text2Loc* significantly outperforms the origin results of Text2Loc, indicating the superiority of modeling the coarse stage as a partially relevant retrieval problem, as well as the proposed CMMT and spatial consolidation scheme. Moreover, CMMLoc_PA and CMMLoc_CDI both have better performance than Text2Loc*, achieving about a 15% improvement at Top-1 on the test set, showing the effectiveness of our proposed modules.

Visualization. We compare our learned embedding space with previous work by T-SNE [39] in Fig. 9. As is shown, Text2Pos [18] and Text2Loc [47] generate less discriminative embedding space, with positive submaps scat-

tered and distant from the query descriptions. In contrast, our method effectively aligns positive submaps with text queries, yielding a more discriminative space for coarse submap retrieval. Moreover, we present some qualitative results in Fig. 8. Given the same text query, we visualize the ground truth, the Top-3 retrieved submaps, and the fine localization results of previous work and ours. Submaps containing the target position are defined as positive. CMMLoc demonstrates superior performance in submap retrieval and localization refinement, not only identifying the positive submaps but also achieving more accurate localization.

6. Conclusion

We analyze existing work on language-based 3D point cloud localization and identify the limitations of the current coarse-to-fine pipeline, namely the neglect of partial relevance between text descriptions and 3D objects and the failure to model this uncertainty. We propose CMMLoc to tackle this problem. In the coarse stage, we are the first to model the task as a partially relevant retrieval problem and propose a Cauchy-Mixture-Model-based Transformer and a spatial consolidation scheme for local modeling of 3D objects and better submap representation. In the fine stage, we enhance fine-grained interactions between texts and objects by pre-aligning text queries with 3D objects and applying a cardinal direction integration module to capture spatial relations between objects. Extensive experiments show that our CMMLoc significantly outperforms the current state-of-the-art, highlighting its effectiveness.

References

- [1] Panos Achlioptas, Ahmed Abdelreheem, Fei Xia, Mohamed Elhoseiny, and Leonidas Guibas. Referit3d: Neural listeners for fine-grained 3d object identification in real-world scenes. In *Computer Vision–ECCV 2020: 16th European Conference, Glasgow, UK, August 23–28, 2020, Proceedings, Part I 16*, pages 422–440. Springer, 2020. 3
- [2] Relja Arandjelovic, Petr Gronat, Akihiko Torii, Tomas Pfister, and Josef Sivic. Netvlad: Cnn architecture for weakly supervised place recognition. In *Proceedings of the IEEE conference on computer vision and pattern recognition*, pages 5297–5307, 2016. 2
- [3] Tiago Barros, Luís Garrote, Ricardo Pereira, Cristiano Prevedida, and Urbano J Nunes. Attdlnet: Attention-based deep network for 3d lidar place recognition. In *Iberian Robotics conference*, pages 309–320. Springer, 2022. 2
- [4] Dave Zhenyu Chen, Angel X Chang, and Matthias Nießner. Scanrefer: 3d object localization in rgb-d scans using natural language. In *European conference on computer vision*, pages 202–221. Springer, 2020. 3
- [5] Shizhe Chen, Pierre-Louis Guhur, Makarand Tapaswi, Cordelia Schmid, and Ivan Laptev. Language conditioned spatial relation reasoning for 3d object grounding. *Advances in neural information processing systems*, 35:20522–20535, 2022. 3
- [6] Youjing Cui and Shuzhi Sam Ge. Autonomous vehicle positioning with gps in urban canyon environments. *IEEE transactions on robotics and automation*, 19(1):15–25, 2003. 1
- [7] Haowen Deng, Tolga Birdal, and Slobodan Ilic. Ppfnet: Global context aware local features for robust 3d point matching. In *Proceedings of the IEEE conference on computer vision and pattern recognition*, pages 195–205, 2018. 2
- [8] Juan Du, Rui Wang, and Daniel Cremers. Dh3d: Deep hierarchical 3d descriptors for robust large-scale 6dof relocalization. In *Computer Vision–ECCV 2020: 16th European Conference, Glasgow, UK, August 23–28, 2020, Proceedings, Part IV 16*, pages 744–762. Springer, 2020. 2
- [9] Zhaoxin Fan, Zhenbo Song, Hongyan Liu, Zhiwu Lu, Jun He, and Xiaoyong Du. Svt-net: Super light-weight sparse voxel transformer for large scale place recognition. In *Proceedings of the AAAI conference on artificial intelligence*, pages 551–560, 2022. 2
- [10] Eduardo Fernández-Moral, Walterio Mayol-Cuevas, Vicente Arevalo, and Javier Gonzalez-Jimenez. Fast place recognition with plane-based maps. In *2013 IEEE International Conference on Robotics and Automation*, pages 2719–2724. IEEE, 2013. 3
- [11] Ross Finman, Liam Paull, and John J Leonard. Toward object-based place recognition in dense rgb-d maps. In *ICRA Workshop Visual Place Recognition in Changing Environments, Seattle, WA*, page 480, 2015. 3
- [12] Dailan He, Yusheng Zhao, Junyu Luo, Tianrui Hui, Shaofei Huang, Aixi Zhang, and Si Liu. Transrefer3d: Entity-and-relation aware transformer for fine-grained 3d visual grounding. In *Proceedings of the 29th ACM International Conference on Multimedia*, pages 2344–2352, 2021. 3
- [13] Yihan Hu, Jiazhi Yang, Li Chen, Keyu Li, Chonghao Sima, Xizhou Zhu, Siqi Chai, Senyao Du, Tianwei Lin, Wenhai Wang, et al. Planning-oriented autonomous driving. In *Proceedings of the IEEE/CVF Conference on Computer Vision and Pattern Recognition*, pages 17853–17862, 2023. 1
- [14] Wencan Huang, Daizong Liu, and Wei Hu. Dense object grounding in 3d scenes. In *Proceedings of the 31st ACM International Conference on Multimedia*, pages 5017–5026, 2023. 3
- [15] Zariah I Kalantan and Jochen Einbeck. Quantile-based estimation of the finite cauchy mixture model. *Symmetry*, 11(9): 1186, 2019. 2
- [16] Giseop Kim and Ayoung Kim. Scan context: Egocentric spatial descriptor for place recognition within 3d point cloud map. In *2018 IEEE/RSJ International Conference on Intelligent Robots and Systems (IROS)*, pages 4802–4809. IEEE, 2018. 2
- [17] Jaeyoung Kim, Mostafa El-Khamy, and Jungwon Lee. Tgsa: Transformer with gaussian-weighted self-attention for speech enhancement. In *ICASSP 2020-2020 IEEE International Conference on Acoustics, Speech and Signal Processing (ICASSP)*, pages 6649–6653. IEEE, 2020. 2, 4
- [18] Manuel Kolmet, Qunjie Zhou, Aljoša Ošep, and Laura Leal-Taixé. Text2pos: Text-to-point-cloud cross-modal localization. In *Proceedings of the IEEE/CVF Conference on Computer Vision and Pattern Recognition*, pages 6687–6696, 2022. 1, 3, 4, 6, 8
- [19] Jacek Komorowski. Minkloc3d: Point cloud based large-scale place recognition. In *Proceedings of the IEEE/CVF Winter Conference on Applications of Computer Vision*, pages 1790–1799, 2021. 2
- [20] Jacek Komorowski, Monika Wysockańska, and Tomasz Trzcinski. Minkloc++: lidar and monocular image fusion for place recognition. In *2021 International Joint Conference on Neural Networks (IJCNN)*, pages 1–8. IEEE, 2021. 2
- [21] Simon Le Cleac’h, Taylor A Howell, Shuo Yang, Chi-Yen Lee, John Zhang, Arun Bishop, Mac Schwager, and Zachary Manchester. Fast contact-implicit model predictive control. *IEEE Transactions on Robotics*, 2024. 1
- [22] Yiyi Liao, Jun Xie, and Andreas Geiger. Kitti-360: A novel dataset and benchmarks for urban scene understanding in 2d and 3d. *IEEE Transactions on Pattern Analysis and Machine Intelligence*, 45(3):3292–3310, 2022. 6
- [23] Zhe Liu, Shunbo Zhou, Chuanzhe Suo, Peng Yin, Wen Chen, Hesheng Wang, Haoang Li, and Yun-Hui Liu. Lpd-net: 3d point cloud learning for large-scale place recognition and environment analysis. In *Proceedings of the IEEE/CVF international conference on computer vision*, pages 2831–2840, 2019. 2
- [24] David G Lowe. Distinctive image features from scale-invariant keypoints. *International journal of computer vision*, 60:91–110, 2004. 2
- [25] Junyu Luo, Jiahui Fu, Xianghao Kong, Chen Gao, Haibing Ren, Hao Shen, Huaxia Xia, and Si Liu. 3d-sps: Single-stage 3d visual grounding via referred point progressive selection. In *Proceedings of the IEEE/CVF Conference on Computer*

- Vision and Pattern Recognition*, pages 16454–16463, 2022. 3
- [26] Junyi Ma, Jun Zhang, Jintao Xu, Rui Ai, Weihao Gu, and Xieyuanli Chen. Overlaptransformer: An efficient and yaw-angle-invariant transformer network for lidar-based place recognition. *IEEE Robotics and Automation Letters*, 7(3): 6958–6965, 2022. 2
- [27] Junyi Ma, Guangming Xiong, Jingyi Xu, and Xieyuanli Chen. Cvtnet: A cross-view transformer network for place recognition using lidar data. *arXiv preprint arXiv:2302.01665*, 2023. 2
- [28] Martin Magnusson, Henrik Andreasson, Andreas Nüchter, and Achim J Lilienthal. Automatic appearance-based loop detection from three-dimensional laser data using the normal distributions transform. *Journal of Field Robotics*, 26(11-12):892–914, 2009. 2
- [29] Charles R Qi, Hao Su, Kaichun Mo, and Leonidas J Guibas. Pointnet: Deep learning on point sets for 3d classification and segmentation. In *Proceedings of the IEEE conference on computer vision and pattern recognition*, pages 652–660, 2017. 2
- [30] Charles Ruizhongtai Qi, Li Yi, Hao Su, and Leonidas J Guibas. Pointnet++: Deep hierarchical feature learning on point sets in a metric space. *Advances in neural information processing systems*, 30, 2017. 4, 1
- [31] Alec Radford, Jong Wook Kim, Chris Hallacy, Aditya Ramesh, Gabriel Goh, Sandhini Agarwal, Girish Sastry, Amanda Askell, Pamela Mishkin, Jack Clark, et al. Learning transferable visual models from natural language supervision. In *International conference on machine learning*, pages 8748–8763. PMLR, 2021. 2
- [32] Colin Raffel, Noam Shazeer, Adam Roberts, Katherine Lee, Sharan Narang, Michael Matena, Yanqi Zhou, Wei Li, and Peter J Liu. Exploring the limits of transfer learning with a unified text-to-text transformer. *Journal of machine learning research*, 21(140):1–67, 2020. 1, 4
- [33] Junha Roh, Karthik Desingh, Ali Farhadi, and Dieter Fox. Languagerefer: Spatial-language model for 3d visual grounding. In *Conference on Robot Learning*, pages 1046–1056. PMLR, 2022. 3
- [34] Timo Röhling, Jennifer Mack, and Dirk Schulz. A fast histogram-based similarity measure for detecting loop closures in 3-d lidar data. In *2015 IEEE/RSJ international conference on intelligent robots and systems (IROS)*, pages 736–741. IEEE, 2015. 2
- [35] Paul-Edouard Sarlin, Cesar Cadena, Roland Siegwart, and Marcin Dymczyk. From coarse to fine: Robust hierarchical localization at large scale. In *Proceedings of the IEEE/CVF conference on computer vision and pattern recognition*, pages 12716–12725, 2019. 2
- [36] Torsten Sattler, Bastian Leibe, and Leif Kobbelt. Efficient & effective prioritized matching for large-scale image-based localization. *IEEE transactions on pattern analysis and machine intelligence*, 39(9):1744–1756, 2016. 2
- [37] Qi Sun, Hongyan Liu, Jun He, Zhaoxin Fan, and Xiaoyong Du. Daggc: Employing dual attention and graph convolution for point cloud based place recognition. In *Proceedings of the 2020 International Conference on Multimedia Retrieval*, pages 224–232, 2020. 2
- [38] Mikaela Angelina Uy and Gim Hee Lee. Pointnetvlad: Deep point cloud based retrieval for large-scale place recognition. In *Proceedings of the IEEE conference on computer vision and pattern recognition*, pages 4470–4479, 2018. 2
- [39] Laurens Van der Maaten and Geoffrey Hinton. Visualizing data using t-sne. *Journal of machine learning research*, 9 (11), 2008. 8
- [40] A Vaswani. Attention is all you need. *Advances in Neural Information Processing Systems*, 2017. 4
- [41] Charles Veach, Patricia McLain, and Michael Murphy. Gps/dead reckoning for vehicle tracking in the “urban canyon” environment. In *Proceedings of VNIS’93-Vehicle Navigation and Information Systems Conference*, pages 461–34. IEEE, 1993. 1
- [42] Guangzhi Wang, Hehe Fan, and Mohan Kankanhalli. Text to point cloud localization with relation-enhanced transformer. In *Proceedings of the AAAI Conference on Artificial Intelligence*, pages 2501–2509, 2023. 1, 3, 4, 6
- [43] Qilong Wang, Banggu Wu, Pengfei Zhu, Peihua Li, Wangmeng Zuo, and Qinghua Hu. Eca-net: Efficient channel attention for deep convolutional neural networks. In *Proceedings of the IEEE/CVF conference on computer vision and pattern recognition*, pages 11534–11542, 2020. 3
- [44] Yuting Wang, Jinpeng Wang, Bin Chen, Ziyun Zeng, and Shu-Tao Xia. Gmmformer: Gaussian-mixture-model based transformer for efficient partially relevant video retrieval. In *Proceedings of the AAAI Conference on Artificial Intelligence*, pages 5767–5775, 2024. 4, 6, 7
- [45] Yanmin Wu, Xinhua Cheng, Renrui Zhang, Zesen Cheng, and Jian Zhang. Eda: Explicit text-decoupling and dense alignment for 3d visual grounding. In *Proceedings of the IEEE/CVF Conference on Computer Vision and Pattern Recognition*, pages 19231–19242, 2023. 3
- [46] Yan Xia, Yusheng Xu, Shuang Li, Rui Wang, Juan Du, Daniel Cremers, and Uwe Stilla. Soe-net: A self-attention and orientation encoding network for point cloud based place recognition. In *Proceedings of the IEEE/CVF Conference on computer vision and pattern recognition*, pages 11348–11357, 2021. 2
- [47] Yan Xia, Letian Shi, Zifeng Ding, Joao F Henriques, and Daniel Cremers. Text2loc: 3d point cloud localization from natural language. In *Proceedings of the IEEE/CVF Conference on Computer Vision and Pattern Recognition*, pages 14958–14967, 2024. 1, 3, 4, 5, 6, 7, 8
- [48] Tian-Xing Xu, Yuan-Chen Guo, Zhiqiang Li, Ge Yu, Yu-Kun Lai, and Song-Hai Zhang. Transloc3d: Point cloud based large-scale place recognition using adaptive receptive fields. *arXiv preprint arXiv:2105.11605*, 2021. 3
- [49] Wenxiao Zhang and Chunxia Xiao. Pcan: 3d attention map learning using contextual information for point cloud based retrieval. In *Proceedings of the IEEE/CVF conference on computer vision and pattern recognition*, pages 12436–12445, 2019. 2
- [50] Wenxiao Zhang, Huajian Zhou, Zhen Dong, Qingan Yan, and Chunxia Xiao. Rank-pointretrieval: Reranking point

cloud retrieval via a visually consistent registration evaluation. *IEEE Transactions on Visualization and Computer Graphics*, 29(9):3840–3854, 2022. [3](#)

- [51] Zhicheng Zhou, Cheng Zhao, Daniel Adolphsson, Songzhi Su, Yang Gao, Tom Duckett, and Li Sun. Ndt-transformer: Large-scale 3d point cloud localisation using the normal distribution transform representation. In *2021 IEEE International Conference on Robotics and Automation (ICRA)*, pages 5654–5660. IEEE, 2021. [2](#)

CMMLoc: Advancing Text-to-PointCloud Localization with Cauchy-Mixture-Model Based Framework

Supplementary Material

A. Overview

In this supplementary material, we provide additional experiments and visualization results to further demonstrate the effectiveness of our proposed CMMLoc. In Sec. B, we conduct an ablation study on our proposed Cauchy-Mixture-Model-based Transformer with different layer numbers on the KITTI360Pose dataset [18], covering both the coarse and fine stages. Moreover, we present the implementation details of our model in Sec. C and more visualization results in Sec. D.

B. More analysis of Cauchy-Mixture-Model-based Transformer

In this section, we primarily analyze the impact of different layer numbers of the proposed Cauchy-Mixture-Model-based Transformer with spatial consolidation scheme on the performance of our CMMLoc, including the coarse submap retrieval stage and the fine localization stage on the KITTI360Pose dataset [18].

For the retrieval of coarse submap, Tab. 5 shows the performance of CMMLoc with different numbers of CMMT-SC, where ‘0’ means that we use the vanilla attention mechanism in Text2Loc [47] instead of our proposed CMMT-SC. As shown, CMMLoc achieves the best performance with a Cauchy-Mixture-Model-based Transformer with spatial consolidation scheme. When the number is set to 2, the performance drops significantly, falling below that of Text2Loc. The performance in fine localization exhibits a similar trend. As shown in Tab. 6, CMMLoc performs best with a single CMMT-SC, but its performance declines sharply when the number is increased to 2.

The possible explanation for the performance degradation when using 2 layers of CMMT-SC is that the heavy-tailed nature of the Cauchy distribution enhances robustness to outliers during modeling. However, applying it consecutively may excessively blur the differences between the original features, thereby reducing the discriminative capability of the model. As a result, we set the fixed number of CMMT-SC as 1 in our CMMLoc.

C. Implementation Details

We conduct our experiments on an NVIDIA A800 GPU. For the coarse submap retrieval, we train the model with Adam optimizer with a learning rate of $5e-4$ for 20 epochs. We set the batch size to 64 and utilize a multi-step training schedule wherein the learning rate is decayed by 0.4 every

Number of CMMT-SC	Submap Retrieval Recall \uparrow					
	Validation Set			Test Set		
	$k = 1$	$k = 3$	$k = 5$	$k = 1$	$k = 3$	$k = 5$
0	0.32	0.56	0.67	0.28	0.49	0.58
1	0.35	0.61	0.73	0.32	0.53	0.63
2	0.31	0.55	0.66	0.27	0.48	0.58

Table 5. Coarse submap retrieval performance for CMMLoc with different numbers of CMMT-SC on the KITTI360Pose benchmark. CMMT-SC denotes the Cauchy-Mixture-Model-based Transformer with spatial consolidation scheme. ‘0’ means using the vanilla attention architecture in Text2Loc [47].

Number of CMMT-SC	Localization Recall ($\epsilon < 5m$) \uparrow					
	Validation Set			Test Set		
	$k = 1$	$k = 5$	$k = 10$	$k = 1$	$k = 5$	$k = 10$
0	0.38	0.69	0.80	0.35	0.63	0.73
1	0.44	0.75	0.83	0.39	0.67	0.77
2	0.39	0.70	0.80	0.35	0.64	0.74

Table 6. Localization performance for Text2Loc with different numbers of CMMT-SC on the KITTI360Pose benchmark. ‘0’ means using the fine localization network from CMMLoc, with submaps retrieved through the coarse submap retrieval framework from Text2Loc [47].

7 epochs. The temperature coefficient τ in the contrastive loss function is set to 0.1. Each submap contains a maximum of 28 objects. We employ PointNet++ [30] in [18] to extract the semantic feature of every object in the submap, followed by a single Cauchy-Mixture-Model-based Transformer with spatial consolidation scheme for local modeling to achieve better submap representation. For the fine localization, we first pre-train the text encoder and object encoder with a learning rate of $3e-4$ with batch size 32 to get a well-initialized state for localization refinement. Then we train the fine localization network with the same learning rate for 45 epochs. For a fair comparison, we set the embedding dimension to 256 for both the text and submap branches in coarse submap retrieval and 128 in fine localization, following the same configuration as in previous work.

D. More Visualization results

In this section, we present additional visualizations to compare our CMMLoc with previous methods, as shown in Fig. 10, including an analysis of a failure case. For (a) and (b), CMMLoc successfully retrieves all positive submaps within the top-3 results during coarse submap retrieval,

Model	Text descriptions	Ground truth	Coarse submap retrieval			Fine localization
			Top 1	Top 2	Top 3	
(a)	Text2Pos The pose is on-top of a gray road. The pose is west of a dark-green building. The pose is east of a beige sidewalk. The pose is east of a beige building. The pose is south of a black pole. The pose is south of a black traffic sign.		 Distance: 6.87	 Distance: n/a	 Distance: 731.57	 Distance: 3.35
	Text2Loc The pose is on-top of a gray road. The pose is west of a dark-green building. The pose is east of a beige sidewalk. The pose is east of a beige building. The pose is south of a black pole. The pose is south of a black traffic sign.		 Distance: 15.46	 Distance: n/a	 Distance: 94.72	 Distance: 22.08
	Ours The pose is on-top of a gray road. The pose is west of a dark-green building. The pose is east of a beige sidewalk. The pose is east of a beige building. The pose is south of a black pole. The pose is south of a black traffic sign.		 Distance: 7.44	 Distance: 6.87	 Distance: 6.71	 Distance: 0.87
(b)	Text2Pos The pose is on-top of a gray building. The pose is east of a gray parking. The pose is north of a green terrain. The pose is east of a gray building. The pose is north of a gray sidewalk. The pose is east of a green vegetation.		 Distance: n/a	 Distance: n/a	 Distance: 424.20	 Distance: n/a
	Text2Loc The pose is on-top of a gray building. The pose is east of a gray parking. The pose is north of a green terrain. The pose is east of a gray building. The pose is north of a gray sidewalk. The pose is east of a green vegetation.		 Distance: 582.78	 Distance: 14.58	 Distance: 430.90	 Distance: 13.57
	Ours The pose is on-top of a gray building. The pose is east of a gray parking. The pose is north of a green terrain. The pose is east of a gray building. The pose is north of a gray sidewalk. The pose is east of a green vegetation.		 Distance: 1.20	 Distance: 8.93	 Distance: 14.58	 Distance: 3.29
(c)	Text2Pos The pose is north of a gray road. The pose is east of a dark-green vegetation. The pose is north of a gray sidewalk. The pose is north of a dark-green fence. The pose is on-top of a gray-green building. The pose is north of a gray-green pole.		 Distance: n/a	 Distance: 300.44	 Distance: n/a	 Distance: n/a
	Text2Loc The pose is north of a gray road. The pose is east of a dark-green vegetation. The pose is north of a gray sidewalk. The pose is north of a dark-green fence. The pose is on-top of a gray-green building. The pose is north of a gray-green pole.		 Distance: 300.44	 Distance: n/a	 Distance: 293.38	 Distance: 299.64
	Ours The pose is north of a gray road. The pose is east of a dark-green vegetation. The pose is north of a gray sidewalk. The pose is north of a dark-green fence. The pose is on-top of a gray-green building. The pose is north of a gray-green pole.		 Distance: 10.91	 Distance: 300.44	 Distance: 293.38	 Distance: 7.43
(d)	Ours The pose is north of a gray road. The pose is on-top of a gray sidewalk. The pose is east of a gray-green parking. The pose is south of a green wall. The pose is west of a dark-green wall. The pose is north of a black sidewalk.		 Distance: 475.53	 Distance: 657.80	 Distance: 469.02	 Distance: 419.01



Figure 10. Qualitative localization results on the KITTI360Pose dataset: In coarse submap retrieval, green boxes indicate positive submaps containing the target location, while red boxes represent negative submaps. For fine localization, red and black dots correspond to the ground truth and predicted target locations. We label the distances between the prediction and ground truth in the submap, with “n/a” indicating submaps from different scenes.

whereas most retrievals from Text2Loc and Text2Pos are incorrect. When the positive submap is retrieved by other methods, our CMMLoc achieves more accurate localization performance. In case (c), although some of the top-3 submaps retrieved by our coarse submap retrieval are negative, CMMLoc effectively localizes the text queries within a 10m range after applying the fine localization network. Moreover, we present a failure case in (d), where all retrieved submaps are negative. In this case, the retrieved submap contains objects with semantic labels and categories that closely resemble those in the ground truth. Consequently, the submap features modeled using the Cauchy Mixture Model are insufficiently discriminative, highlighting the importance of developing more robust representations to better distinguish between submaps.